Methods 63 (2013) 255–265

Contents lists available at ScienceDirect

Methods

journal homepage: www.elsevier.com/locate/ymeth

Functional nucleic acid entrapment in sol–gel derived materials

Carmen Carrasquilla, John D. Brennan *

Department of Chemistry and Chemical Biology, McMaster University, Hamilton, Ontario L8S 4M1, Canada

ARTICLE INFO

Article history:
Available online 8 September 2013

Keywords:
Nucleic acid
Aptamer
Deoxyribozyme
Fluorescence
Sol–gel process
Immobilization
Entrapment
Biosensor

ABSTRACT

Functional nucleic acids (FNAs) are single-stranded DNA or RNA molecules, typically generated through *in vitro* selection, that have the ability to act as receptors for target molecules (aptamers) or perform catalysis of a chemical reaction (deoxyribozymes and ribozymes). Fluorescence-signaling aptamers and deoxyribozymes have recently emerged as promising biological recognition and signaling elements, although little has been done to evaluate their potential for solid-phase assays, particularly with species made of RNA due to their lack of chemical stability and susceptibility to nuclease attack. Herein, we present a detailed overview of the methods utilized for solid-phase immobilization of FNAs using a sol–gel entrapment method that can provide protection from nuclease degradation and impart long-term chemical stability to the FNA reporter systems, while maintaining their signaling capabilities. This article will also provide a brief review of the results of such entrapment studies involving fluorescence-signaling versions of a DNA aptamer, selected RNA-cleaving deoxyribozymes, and two different RNA aptamers in a series of sol–gel derived composites, ranging from highly polar silica to hydrophobic methylsilsesquioxane-based materials. Given the ability to produce sol–gel derived materials in a variety of configurations, particularly as thin film coatings on electrodes, optical fibers, and other devices, this entrapment method should provide a useful platform for numerous solid-phase FNA-based biosensing applications.

1. Introduction

Advances in nucleic acid technology have expanded the range of biomolecules for sensing applications through the generation of functional nucleic acids (FNAs). These include single-stranded DNA or RNA molecules that can function as receptors for target molecules or as catalysts for chemical reactions owing to their ability to fold into distinct three-dimensional structures [1,2]. An advantage of FNAs is that they can be generated by *in vitro* selection from large random-sequence or semi-rationally designed libraries containing up to 10^{16} unique molecules, allowing for identification of sequences that exhibit desired functionalities such as ligand binding or catalytic activity [3–6]. Thus, hundreds of aptamers that function as receptors for a variety of targets (including proteins, small metabolites or even cells) with high specificity and affinity [7], as well as (deoxy)ribozymes (also known as DNA/RNA enzymes, DNA/RNAzymes or catalytic DNA/RNA) with catalytic capabilities such as cleavage of RNA substrates, autophosphorylation, and porphyrin metallation [8,9] have been generated in recent years. Moreover, RNA-based aptamers and enzymes have also been derived from natural sources (i.e. riboswitches and ribozymes, respectively) [10–13].

The chemical stability of DNA and ease of site-specific modification of nucleotides for signal-development have revealed the potential of DNA-based FNAs as desirable alternatives to traditional protein-based enzymes and antibodies for use as biological recognition elements in analytical and diagnostic applications [14–16]. However, the limited range of analytes for DNA aptamers (with only ~50 targets as of 2009) [1] and the lack of known naturally-evolved DNA aptamers limit their potential for widespread use in sensing applications.

RNA aptamers, by contrast, can fold into more complex structures in order to provide a greater diversity of potential analytes, as demonstrated by the existence of over one hundred unique RNA aptamers for various small-molecule and protein targets [7,17]. However, reports on the use of RNA-based aptamers in solution or solid-phase biosensing applications are still relatively limited, mostly due to their inherent chemical instability and susceptibility to nuclease attack [18–20].

To address the signaling ability of DNA and RNA-based aptamers, the Li group developed a structure-switching/fluorescence-signaling reporter system [21,22]. In this approach, complementary fluorophore-labeled DNA (cFDNA) and quencher-labeled DNA (cQDNA) strands are designed to hybridize adjacent to one another on the aptamer sequence (APT) to create a tripartite construct. Switching conformations from an aptamer/DNA duplex to an aptamer/target complex is thus coupled to a fluorescence-dequenching mechanism that generates a fluorescence signal due

* Corresponding author. Fax: +1 905 527 9950.
E-mail address: brennanj@mcmaster.ca (J.D. Brennan).
URL: http://www.chemistry.mcmaster.ca/faculty/brennan (J.D. Brennan).

1046-2023/$ - see front matter © 2013 Elsevier Inc. All rights reserved.
http://dx.doi.org/10.1016/j.ymeth.2013.08.035

to displacement of the cQDNA upon target binding. Bipartite constructs can also be designed using a fluorophore-labeled aptamer strand and cQDNA as seen in Fig. 1.

Real-time fluorescence signal generation by means of dequenching due to (deoxy)ribozyme catalysis can function similarly through the incorporation of strategically placed fluorophore–quencher pairs. This technique has been widely used with the most common type of deoxyribozymes reported to date, which catalyze cleavage of a single RNA linkage within a DNA substrate [23,24]. High signal enhancements are observed when using fluorophore–quencher pairs situated immediately on either side of the scissile phosphodiester linkage due to their close proximity prior to cleavage [25–27]. Since DNAzymes require specific divalent metal ion cofactors to induce the formation of a catalytic site that cleaves the RNA linkage, these fluorescence signaling DNAzymes can be used as metal ion sensors [28].

The employment of FNA reporters for solid-phase biosensing applications relies on their immobilization on or within a suitable surface while maintaining chemical stability and structure-switching abilities [29]. Typical methods used to immobilize nucleic acids are based on surface attachment via covalent, electrostatic or affinity interactions [30,31]. Physical adsorption can result in the DNA molecules being immobilized in a random orientation, which may reduce activity, increase dissociation from the surface or make them inaccessible to their target [32]. Although the use of covalent or affinity interactions offers greater control over orientation [33], these methods may still suffer from poor sensitivity due to low packing density, steric effects that reduce activity, the incorporation of functional groups for immobilization, and lack of protection against nuclease degradation [31,34].

An alternative route for bio-immobilization involves entrapment of nucleic acids within three-dimensional matrices of porous silica or organosilane composite materials using the sol–gel process [35,36]. Typically, this is a two-step process that begins with the hydrolysis of a suitable silane precursor to form an aqueous "sol". This hydroxysilane is then mixed with a buffered aqueous solution containing the biomolecules of interest. The sudden change in ionic strength and more neutral (physiological) pH, results in condensation and polycondensation of the silane, forming siloxane bonds that entrap the biomolecules within the nanoscale pores of the cross-linking gel matrix. Thus, using this method, biomolecules are not bound to the support surface but are retained through size-exclusion, while small analyte molecules may diffuse into the region containing the biosensing species. Indeed, this simple immobilization process has been shown to be "biofriendly" and applicable to the entrapment of a variety of viable biomolecules [37,38], including soluble and labile membrane-bound proteins, suggesting that the method should be useful for solid-phase immobilization of FNAs.

In this review, we provide selected examples from our research group to demonstrate the protocols used for FNA entrapment in a variety of sol–gel processed materials (polar, anionic, cationic, hydrophobic), the methods used to assess and characterize FNA reporter function in the materials, and the advantages of solid-phase sensor design offered by entrapping signaling FNAs in sol–gel derived materials (Fig. 2). The entrapped FNA reporters studied include a structure-switching DNA aptamer for binding adenosine 5′-triphosphate (ATP) [39], various divalent metal ion-dependent deoxyribozymes that catalyze RNA cleavage [40] and two different structure-switching RNA aptamers: the synthetic theophylline-binding aptamer and a thiamine pyrophosphate (TPP)-binding riboswitch [41]. Following the description of these methods, we summarize the resulting data, which clearly show retention of their signaling capabilities in optimized materials, along with protection from nuclease degradation and improved long-term stability of the entrapped FNA reporter systems. Moreover, since the types of materials in which the FNAs function optimally have also shown amenability for protein immobilization, a co-entrapment assay that uses a signaling DNA aptamer to report the activity of a protein enzyme [42] is briefly discussed as one example of the many possible applications for sol–gel-based entrapment of FNA reporter systems for solid-phase biosensing.

2. List of materials

2.1. Preparation protocol

2.1.1. DNA oligonucleotides

For the experiments described herein, the fluorescence-signaling FNAs used are:

1. Tripartite ATP-binding DNA aptamer [21].
2. Bipartite ATP-binding DNA aptamer [39].
3. OA-II RNA-cleaving deoxyribozyme for Mg(II) and Ni(II) [26].
4. OA-III RNA-cleaving deoxyribozyme for Mn(II) only [26].
5. OA-IV RNA-cleaving deoxyribozyme for Mn(II) and Cd(II) [26].
6. Synthetic theophylline-binding RNA aptamer [22].
7. Naturally-occurring TPP-binding RNA aptamer [22].

The sequences of the all DNA oligonucleotides are given in Table 1, including the locations of the fluorescein (**F**) and DABCYL (4-(4-dimethylaminophenylazo)benzoic acid) quencher (**Q**) labels.

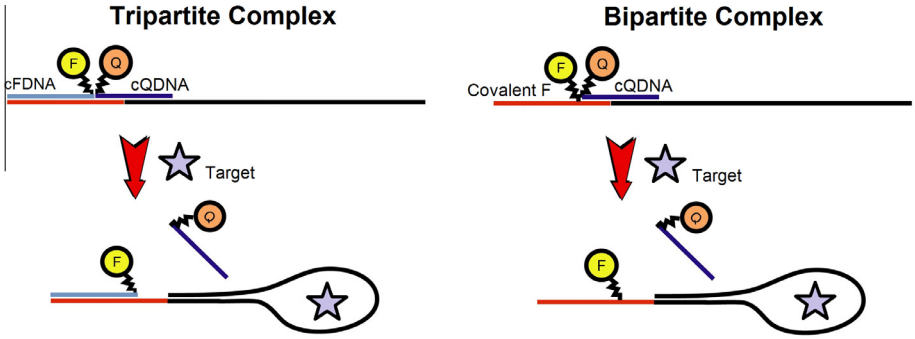

Fig. 1. Schematic of the structure-switching signaling aptamer constructs. The tripartite complex (left) is composed of three separate strands: cFDNA, cQDNA and the aptamer. Both the cFDNA and cQDNA are complementary to the aptamer or its sequence extension. In the bipartite scheme (right), the construct consists of the cQDNA and aptamer strand with a covalently tethered fluorophore. Upon target addition, the aptamer undergoes a conformational change, which displaces the cQDNA and results in a fluorescence signal.

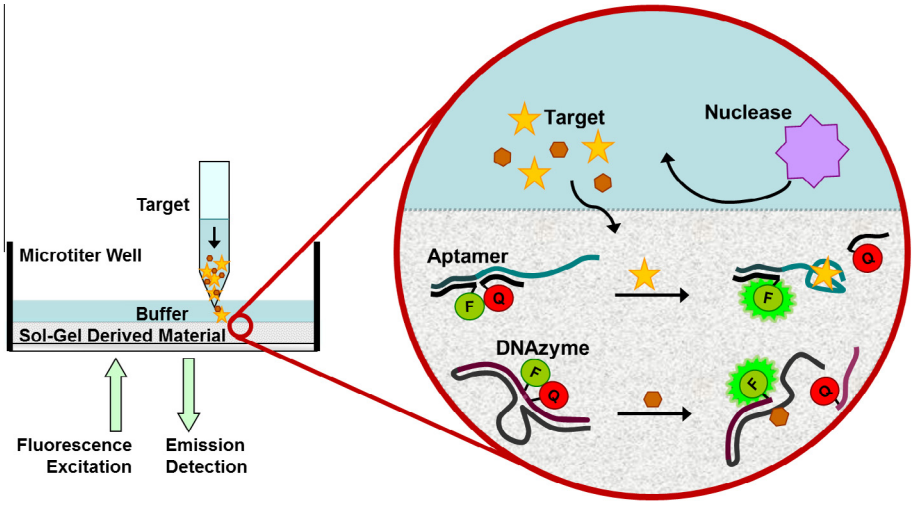

Fig. 2. Schematic of the two different classes of functional nucleic acid reporter systems entrapped in a sol–gel derived matrix and detection of their fluorescence signal from a microtiter plate.

Table 1
DNA oligonucleotide sequences for FNA reporter systems.

DNA oligonucleotide	Sequence (5′ → 3′)
ATP aptamer[a]	CCTGC CACGC TCCGC TCACT GACCT GGGGG AGTAT TGCGG AGGAA GGT
ATP aptamer cFDNA	**F**GCGGA GCGTG GCAGG
Fluorescein-labeled ATP aptamer[b]	TTTTT TTTTT**F** TCACT GACCT GGGGG AGTAT TGCGG AGGAA GGT
ATP aptamer cQDNA	CCCAG GTCAG TG**Q**
cis-Acting DNAzyme substrate	TTTGT GTCCG TGC**Fr*A***G**Q** GTTCG ATCAA G
cis-Acting DNAzyme OA-II[c]	ATTGC ACTTG ATCGA GTTCC GGTCT CGAGG GCGTA GCCAC ACGGA C
Ligation template for OA-II	ATCTG CAATC TTGAT CGAAC CATAG C
cis-Acting DNAzyme OA-III	ATTGC AGATC GAACC CATTA TGATC CGTAG GAGGA AGAGG GACA
Ligation template for OA-III	ATCTG CAATC TTGAT CGAAC CATAG C
cis-Acting DNAzyme OA-IV[d]	GACAT TGAAC CAGTC TGTAA GACCA AGGCT GGCGG GAGGA TGCAC GGAC
Ligation template for OA-IV	TTCAA TGTCC TTGAT CGAAC CATAG C
DNA template for theophylline reporter[e,f]	GAATT CTAAT ACGAC TCACT ATAGG CCTGC CACGC TCCGA CGCTA TCACT CTATG GGCGA TACCA GCCGA AAGGC CCTTG GCAGC GTCCA ACACA TCG
Theophylline aptamer template forward primer	GAATT CTAAT ACGAC TCACT ATA
Theophylline aptamer template reverse primer	CGATG TGTTG GACGC
DNA template for the TPP reporter[g,h]	GAATT CTAAT ACGAC TCACT ATAGG CCTGC CACGC TCCGA CGCTA TCACT CTATG CCACT AGGGG TGCTT GTTGT GCTGA GAGAG GAATA ATCCT TAACC CTTAT AACAC CTGAT CTAGG TAATA CTAGC GAAGG GAAGT GG
TPP aptamer template forward primer	GAATT CTAAT ACGAC TCACT ATA
TPP aptamer template reverse primer	GCTTC TGTTC CCACT
Theophylline/TPP aptamer cFDNA	**F**TAGCG TCGGA GCGTG GCAGG
Theophylline aptamer cQDNA	TATCG CCCAT AGAGT G**Q**
TPP aptamer cQDNA	CTAGT GGCAT AGAGT G**Q**

[a] Mutant was made by replacing T_{35} and G_{43} with A_{35} and C_{43}.
[b] Mutant was made by replacing G_{25} and G_{37} with T_{25} and T_{37}.
[c] Mutant was made by replacing G_{21} with T_{21}.
[d] Mutant was made by replacing G_{28} with T_{28}.
[e] Mutant 1 template was made by replacing C_{64} and A_{83} with A_{64} and T_{83}.
[f] Mutant 2 template was made by replacing $C_{63}C_{64}$ with $G_{63}A_{64}$.
[g] Mutant 1 template was made by replacing G_{60}, G_{74}, G_{76}, A_{77} and G_{126} with C_{60}, C_{74}, T_{66}, T_{67}, T_{126}.
[h] Mutant 2 template was made by replacing G_{60}, T_{73},G_{74}, G_{76}, A_{77}, C_{125}, G_{126}, G_{131}, A_{132} with C_{60}, C_{73}, C_{74}, T_{66},T_{67}, A_{125}, T_{126}, C_{131}, G_{132}.

In the DNAzyme substrate sequence, ***rA*** refers to an adenine ribonucleotide.

Purified water (18.2 MΩ cm, 1–5 ppb solids) from a Milli-Q water purification system is used in all experiments. Enzymes and their buffers as well as nucleotides are purchased from Fermentas Life Sciences (Burlington, ON) while other chemicals are obtained from Sigma–Aldrich (Oakville, ON) unless otherwise stated.

2.1.2. Ligation of DNAzymes with substrates

- T4 polynucleotide kinase (PNK).
- 10× reaction buffer A (for forward reaction; 500 mM Tris·HCl, 100 mM $MgCl_2$, 50 mM DTT, 1 mM spermidine at pH 7.6).
- T4 DNA ligase.
- 10× DNA ligase buffer (400 mM Tris·HCl, 100 mM $MgCl_2$, 100 mM DTT, 5 mM ATP at pH 7.8).
- ATP.
- Tetrabutylammonium fluoride (TBAF) solution.
- Sodium dodecyl sulfate (SDS).
- Tris(hydroxymethyl)aminomethane.
- Nanosep® 3 K Omega spin column (Pall Corp., Ann Arbor, MI).

2.1.3. RNA aptamer transcription

- *Taq* DNA polymerase (Biotools, Madrid, Spain).
- 10× standard reaction buffer with $MgCl_2$ (750 mM Tris·HCl, 500 mM KCl, 200 mM $(NH_4)_2SO_4$, 20 mM $MgCl_2$ at pH 9.0; Biotools).
- Deoxyribonucleoside triphosphate (dNTP) set.
- Ribonucleoside triphosphate (NTP) set.
- T7 RNA polymerase.
- 5× transcription buffer (200 mM Tris·HCl, 30 mM $MgCl_2$, 50 mM DTT, 50 mM NaCl, 10 mM spermidine at pH 7.9).
- Deoxyribonuclease I (DNase I).

2.1.4. Preparation of sol–gel derived materials

- Glycerol (anhydrous, ~99.5%).
- Dowex 50 × 8–100 cation exchange resin.
- Hydrochloric acid concentrate (HCl, 0.1 N).
- Sodium silicate solution (SS solution; purum, ~10% Na_2O, ~27% SiO_2).
- Tetramethyl orthosilicate (TMOS).
- Methyltrimethoxysilane (MTMS).
- (3-Aminopropyl)triethoxysilane (APTES).
- Diglycerylsilane (DGS; prepared from TMOS in-house, see below).
- Acrodisc® syringe filter: 0.2 μm, 0.45 μm (Pall Corp.).

2.1.5. Preparation of FNA reporter complexes

- DNA aptamer assay buffer: 20 mM Tris·HCl, 100 mM NaCl and 5 mM $MgCl_2$ at pH 7.8.
- Deoxyribozyme assay buffer: 50 mM HEPES at pH 6.8 (for OA-II); 50 mM HEPES at pH 7.5 (for OA-III); 50 mM HEPES, 100 mM KCL at pH 7.5 (for OA-IV).
- RNA aptamer assay buffer: 50 mM Tris·HCl, 20 mM $MgCl_2$ at pH 7.5.

2.2. Assay procedure

2.2.1. Sol–gel derived materials screen

- For ATP-binding DNA aptamer: 2 mM ATP.
- For metal ion-binding deoxyribozymes: 1 mM $MgCl_2$ and 0.1 mM $NiCl_2$ (for OA-II); 2 mM $MnCl_2$ (for OA-III); 1 mM $MnCl_2$ and 0.1 mM $CdCl_2$ (for OA-IV).
- For theophylline-binding RNA aptamer: 1 mM theophylline.
- For thiamine-binding RNA aptamer: 100 μM TPP.

2.2.2. Sensitivity and selectivity assays

- For ATP-binding DNA aptamer: cytosine 5′-triphosphate (CTP), guanosine 5′-triphosphate (GTP), uridine 5′-triphosphate (UTP).
- For metal ion-binding deoxyribozymes: $MnCl_2$, $CdCl_2$, $CoCl_2$ (for OA-II); $MgCl_2$ $NiCl_2$, $CdCl_2$, $CoCl_2$ (for OA-III); $MgCl_2$, $NiCl_2$, $CoCl_2$ (for OA-IV).
- For theophylline-binding RNA aptamer: theobromine, caffeine.
- For thiamine-binding RNA aptamer: thiamine monophosphate (TMP), thiamine, oxythiamine.

2.2.3. Nuclease degradation studies

- DNase I.
- Ribonuclease A (RNase A).
- Ribonuclease H (RNase H).
- Streptavidin-coated 96-well multiwall plate (NoAb Biodiscoveries Inc., Mississauga, ON).

2.2.4. Cointrapment assays

- Adenosine.
- Adenosine deaminase (ADA; from Sigma–Aldrich).
- Erythro-9-(2-hydroxy-3-nonyl)adenine (EHNA) hydrochloride.

3. Description of methods

3.1. Preparation protocol

3.1.1. DNA oligonucleotide synthesis and purification

All DNA oligonucleotides are synthesized using standard phosphoramidite chemistry by Integrated DNA Technologies (Coralville, IA). Fluorescently-labeled DNA sequences are purified by HPLC, while unmodified oligonucleotides are purified by 10% denaturing (8 M urea) polyacrylamide gel electrophoresis (PAGE), followed by elution, ethanol precipitation, and quantification by absorbance at 260 nm prior to use. Detailed descriptions of these procedures are described in another *Methods* article from the Li group [43].

3.1.2. Ligation of DNAzymes with substrates

The *cis*-acting DNAzymes (OA-II, OA-III, and OA-IV) are produced by ligating the substrate sequence, containing the adenine ribonucleotide flanked by a fluorophore–quencher pair, with a relevant 5′-phosphorylated DNAzyme sequence using a matching ligation template (to ensure substrate proximity to the catalytic core). All three DNAzymes were optimized from a single selection pool for the same substrate strand under different metal ion conditions [26], increasing ease and cost-efficiency in constructing a single dual-labeled substrate for different DNAzymes. Note: these same DNAzymes can also function in *trans*, with the substrate as a separate strand, but this requires extending the number of base pairs hybridizing the 3′-end of the substrate with the DNAzyme to create a stable helix.

Phosphorylation reactions are performed in 1× reaction buffer A (diluted from 10× reaction buffer) with 0.1 units/μL PNK, 1 mM ATP, and 400 pmol DNAzyme sequence at 37 °C for 30 min followed by heating at 90 °C for 5 min to inactivate the enzyme. Once cooled to room temperature, 400 pmol substrate and 0.05 units/μL T4 DNA ligase in 1× DNA ligase buffer are added and incubated at 25 °C for 12 h, followed by enzyme inactivation 90 °C for 5 min.

The TOM (triisopropylsisyloxymethyl) protecting group on the 2′-hydroxyl group of the RNA linkage is removed by incubation with 150 μL of TBAF solution at 60 °C with shaking for 6 h, followed by the addition of 250 μL of 100 mM Tris·HCl (pH 8.3) and further shaking at 37 °C for 30 min. The DNA is recovered using ethanol precipitation, dissolved in water containing 0.1% SDS, and the tetrabutylammonium salt is removed by centrifugation using the Nanosep® spin column.

3.1.3. RNA aptamer transcription

Aptamer sequences made of RNA are prepared by *in vitro* transcription using aptamer-encoded DNA templates for ease of synthesis and cost efficiency. Polymerase chain reaction of the DNA templates for the theophylline and TPP aptamer is conducted in 1× standard reaction buffer (from the 10× standard reaction buffer) with 0.5 μM primer, 3 nM template, 0.5 mM of each dNTP and 5 units of *Taq* DNA polymerase. Thermal cycling steps are: 94 °C for 1 min, 20 cycles of 94 °C–45 °C–72 °C for 30 s each, and 72 °C for 8 min.

The transcription reactions are conducted at 37 °C for 2 h in 150 μL of 1× transcription buffer with 25 pmol PCR amplified DNA, 2.5 mM of each NTP and 1.5 units/μL T7 RNA polymerase. The transcription mixture is then treated with 3 units of DNase I for 30 min at 37 °C to degrade the DNA templates and the transcribed RNA purified by 10% denaturing PAGE and quantified spectroscopically.

3.1.4. Synthesis of DGS precursor

Diglycerylsilane precursor is prepared in-house beginning with the transesterification of TMOS with glycerol by mixing neat TMOS (24.2 mL, 0.164 mol) and anhydrous glycerol (25.4 mL, 0.348 mol) in a round-bottom flask and heating with an oil bath at 60 °C, with a fractionating (Vigreux) column and short-path distillation head with jacketed condenser in place under N_2, and increasing 20 °C each hour until a temperature of 105 °C is reached and the solution is homogenous (~3 h). Following this, insulation is added around the column and the methanol is slowly distilled off at 120 °C for 18–20 h. Further distillation and drying *in vacuo* at 130 °C for 1 h, using only the distillation head with condenser, allows complete removal of residual methanol and unreacted starting materials to produce uncontaminated DGS.

After allowing the reaction to cool to room temperature, the remaining hard white solid is broken up and stored in many small N_2-purged vials in a desiccator. Since hydrolysis competes to form polyglycerylsilanes, it is imperative that anhydrous conditions are maintained throughout synthesis and storage and the purity of the DGS product should be confirmed by solid state MAS ^{29}Si- and ^{13}C-NMR. Additional details on the preparation and characterization of DGS are given elsewhere [44,45].

3.1.5. Preparation of sol–gel derived materials

A series of sol–gel derived materials were assessed as potential materials for FNA entrapment, including those prepared from two previously reported biofriendly precursors (SS and DGS) with and without APTES (to produce a cationic surface), along with TMOS-derived composites containing up to 80% MTMS to produce a gradient of polarity, and hydrophobic methylsilsesquioxane (MSQ) materials derived from pure MTMS. Owing to the ability of DNA to withstand ethanol precipitation with recovery of function after placement in water we were not concerned about the effect of alcohol byproducts of organosilane hydrolysis (though this is a major issue for protein entrapment [46]), allowing these "less biofriendly" alkoxysilanes to be included in our evaluation of materials.

Sodium silicate sols are prepared by diluting 2.6 g of a stock SS solution to 10 mL with water, immediately mixing the solution with 5.5 g Dowex for 1 min to bring the pH of the SS solution to ~4, and then vacuum filtering this solution through a Büchner funnel to remove the Dowex resin followed by further filtration through a 0.45 μm membrane syringe filter to remove any particulates in the solution. Before use, 120 g of the Dowex resin is cleaned with 150 mL 0.1 N HCl and stirring for 1 h, followed by vacuum filtration and washing with water until the filtrate runs clear. It is very important to ensure that the final pH of the sol solution is close to 4.0, otherwise the final material will not form optimal materials.

The DGS sol is prepared by grinding DGS precursor to a fine powder and dissolving 0.5 g in 1 mL of water, followed by 15 min sonication in ice-cold water and filtering the solution through a 0.2 μm membrane syringe filter. These sols should be used immediately. Materials containing 0.1% (v/v) APTES in either SS or DGS are made by adding APTES to the sol prior to addition of buffered FNA solutions.

To make TMOS and MTMS sols, 700 μL of water and 50 μL HCl (0.1 N) are added to 2.25 mL TMOS or MTMS and then sonicated for 20 min in ice-cold water. The TMOS–MTMS mixtures are prepared by proportionally dividing the 2.25 mL of silane using volume percentages of 20–80% MTMS in TMOS (in 20% increments), mixing with water and acid and co-hydrolyzing in a sonicator as described above. All prepared sols should be stored on ice until use (and used within the hour).

3.1.6. Characterization of sol–gel derived materials

The physical properties of the sol–gel derived materials are generally characterized by a variety of methods in order to establish the compositions of materials that provide an optimal environment for FNA entrapment. For these characterization studies, larger monoliths (3 mL total volume of 1:1 sol–gel precursor:buffer, v:v) of the various sol–gel derived materials described above are prepared in order to have sufficient material for the measurements described below. After gelation, monoliths are cured in air for 4–6 h at room temperature prior to aging for 5 days in sealed vials.

In order to assess the polarity of materials, water contact angle measurements are performed using a Krüss drop shape analyzer system (DSA10, Dataphysics) at 22 °C by applying conventional sessile drops on the material surface. Average contact angle is calculated from three values obtained in different areas of each sample.

For mesopore size distribution data, samples are desiccated for another 7 days. Nitrogen sorption measurements of the dried, crushed monoliths are performed with a Quantachrome Nova 2000 surface area/pore size analyzer (Boca Raton, USA). At least 50 mg of each sample is evacuated to 0.1 Torr and heated at 120 °C for 6 h to remove air and residual water from the surface. Pressure is measured as nitrogen is adsorbed and desorbed at a constant temperature of −196 °C. Surface area can be calculated by the BET (Brunauer, Emmett and Teller) equation and the average pore size and distribution of pore sizes (from the desorption branch) is calculated using the BJH (Barrett, Joyner and Halenda) method using the software provided with the instrument. Mercury intrusion porosimetry measurements are used to determine macropore properties, and are performed using a Quantachrome Poremaster® GT mercury intrusion porosimeter (Boca Raton, USA) with ~100 mg of each sample. The contact angle is 140°, running a fixed speed pressure gradient from 1.4 to 4195 kg cm^{-1}. Median pore diameters, bulk particle density and percent porosity are determined as a function of intruded volume using the software provided by Quantachrome. It is important to note that the methods used to prepare samples for nitrogen and mercury porosimetry (i.e., heating, degassing) generally cause a reduction in pore size relative to the hydrated samples, hence porosimetry is best used to compare relative pore sizes between different materials rather than to ascertain pore sizes of functional, hydrated materials.

For morphology visualization, samples for SEM imaging are aged for 10 days before analysis and coated with 5 nm of platinum under vacuum to improve conductivity. Imaging is performed at 5 kV using a JEOL JSM 7000F Scanning Electron Microscope.

3.1.7. Preparation of FNA reporter complexes

Stock solutions of the various FNA components are prepared at a concentration of 10 μM in water. For RNA studies, buffer solutions are autoclaved after preparation to ensure that no active nucleases are present. The tripartite complexes of the aptamer reporters are prepared by combining cFDNA, APT, and cQDNA in a 1:2:3 M ratio in the appropriate buffer, incubating for at least 1 h at 25 °C to ensure annealing/quenching and storing at 4 °C until analysis. For studies involving RNA aptamers, this mixture is first heated at 65 °C for 2 min to eliminate any self-complementation of the aptamer strand (allowing for optimal cFDNA and cQDNA hybridization), cooled at room temperature for 10 min, and then stored. The ratios of 1:2:3 the three components ensures adequate quencher is present to significantly reduce fluorescence intensity upon hybridization of all species. However, it is recommended that

optimization of cFDNA:APT:cQDNA be done for each aptamer system to maximize signal enhancement upon target binding.

To create the bipartite complex, the labeled aptamer strand (F-APT) and the cQDNA are combined in a 1:3 M ratio in the appropriate buffer (to ensure that the fluorophore/quencher ratio are the same as in the tripartite system). Signaling DNAzymes are diluted in the appropriate buffer after being ligated to their substrate sequence. Final concentrations of aptamers and DNAzymes both in solution and entrapped in materials are 80 nM and 250 nM, respectively (these concentrations provide sufficient signal levels and allow direct comparison to previous FNA reporter studies in solution that used similar concentrations for fluorescence detection).

3.1.8. Entrapment of FNA reporter complexes

The FNA mixture solutions for entrapment are prepared at double the concentration of typical solutions in double concentration (2×) buffer. These buffered FNA solutions are then stored at 4 °C until mixing in a 1:1 (v:v) ratio with a freshly-prepared silica sol at room temperature. The FNA–sol mixtures are deposited into microtiter plates at a volume of 50 μL per well (96-well plate) or 15 μL per well (384-well plate) and allowed to gel (typically 5 min–1.5 h, depending on the sol composition, as determined by loss of ability to flow when the plate is tilted). The materials in the plates are left to age in air at 4 °C for at least 2 h and then overlaid with 50 μL or 15 μL of the appropriate buffer for storage before analysis (for 96-well and 384-well plates, respectively).

3.2. Factors affecting entrapped FNA activity

Proper performance of any entrapped fluorescence-signaling FNA requires that (i) the fluorophore- and quencher-labeled strands remain fully hybridized/intact upon entrapment to ensure low background prior to target addition, (ii) the FNA does not leach out from the matrix, and (iii) the FNA remains accessible to externally added target molecules for recognition/binding. Additionally, each FNA should also retain enough conformational flexibility to undergo the structural switch necessary for correct folding (of a recognition or catalytic site) upon target binding, and the QDNA should be able to move far enough from the FNA to produce a large fluorescent signal increase. Thus, an optimal material for FNA entrapment should provide the highest overall signal and most rapid signal evolution, while also conferring benefits such as protection from degradation to provide the long-term stability that is required of a viable and robust biosensor. Below we describe the procedures for evaluating FNA properties and performance when entrapped in sol–gel derived materials by first optimizing the choice of entrapment material for minimal leaching and maximal signaling, followed by more extensive studies of the FNA performance using only these optimal materials (Fig. 3).

3.3. Fluorescence detection

All DNA aptamer and DNA enzyme studies are performed at 25 °C, while those involving the RNA aptamers are performed at 37 °C, using a Tecan Infinite® M1000 platereader (San Jose, CA) operated in fluorescence mode. We have found that black plates with flat, clear bottoms provide the lowest background for these fluorescence studies. However, before running assays, full emission scans (2-nm increment, 500–650 nm emission) should be performed to assess the maximal fluorescence emission wavelength of reporters under varying buffer conditions and any effects of background signals. Moreover, samples must also be corrected for light scattering by blank subtraction of signals originating from the materials or from buffer without entrapped FNA reporters present; failure to do so produces artificially low fluorescence enhancements upon target binding. Finally, it is important to avoid the outermost ring of wells, as these produce fluorescence signals that are not within error of those obtained from inner wells. In all the following experiments, both solution and entrapped FNA samples are excited at 490 nm with emission collected at 520 nm using a 5-nm bandpass for both excitation and emission and a 0.5 s integration time using the bottom-read setting, as these parameters demonstrate the highest signals with the lowest background levels.

Kinetic measurements are performed to assess FNA response to addition of given species (i.e. targets, nucleases, etc.) using fluorescence intensity reads every 1 min for both baseline measurements (no target; typically 5–10 min) and after addition of targets/nucleases for a total of at least 60 min, with orbital shaking of 2.5 mm amplitude for 2 s between each measurement to ensure proper mixing.

For ease of comparison, raw fluorescence measurements can be normalized to fluorescence enhancement or F/F_o where F is the endpoint fluorescence intensity and F_o is the initial fluorescence intensity at time = 0 prior to target addition. In some cases (for example, with measurements involving metal ion analytes that quench fluorescence at higher concentrations), when the endpoint fluorescence intensity does not equal the maximal fluorescence, i.e. the intensity reaches a plateau and subsequently decreases, F may refer to the maximal enhancement reached during plateau and not the final intensity.

Dynamic response data (i.e., initial rates) can also be used to indicate signaling efficiency and can be determined from kinetic measurements by calculating the initial slope of the response (change in fluorescence versus time) over the first few minutes after addition of target (more than three measurements within the linear range) and thus, also leads to a shorter analysis time since it is not necessary to wait until a steady-state signal is reached.

Fluorescence images of microwell plates can also be acquired using a Typhoon Trio+ Variable Mode Imager (Molecular Dynamics, Sunnyvale, CA) with excitation at 488 nm, 526 nm emission collection, medium sensitivity and 100 micron resolution. Quantitative data can be obtained from pixel intensity values calculated using software supplied with the system. To avoid the need to acquire two separate fluorimages, an appropriate blank (no target or mutant FNA sequence) made in the same plate can be used for subtraction of blanks.

3.4. Assay procedure

3.4.1. Leaching of FNA species

Prior to any fluorescence assays, the various sol–gel derived materials containing the reporter complexes are washed three times with buffer at room temperature using a plate shaker for ~10 min per wash to remove any un-encapsulated FNA from the material surface beforehand. The percentage of FNA leached can be determined by comparing the total fluorescence intensity of the materials prior to a washing step with that of the materials after each wash, being careful to ensure identical pH and ionic strength conditions. Each wash solution can also be added to an empty well and measured to ensure that the intensity correlates well with the changes in fluorescence intensity from the material.

3.4.2. Sol–gel derived materials screen

The performance of the FNA reporter system must be examined (using binding assays) both for FNA that is in solution and for species entrapped in the full series of sol–gel derived materials to determine an optimal material for entrapment of a particular FNA. The target concentrations listed above in Section 2.2.1 represent the "100% concentration" to induce maximal fluorescence signaling of each FNA in solution (note: in DNAzyme solution assays, the optimal metal ion concentration for maximal signal

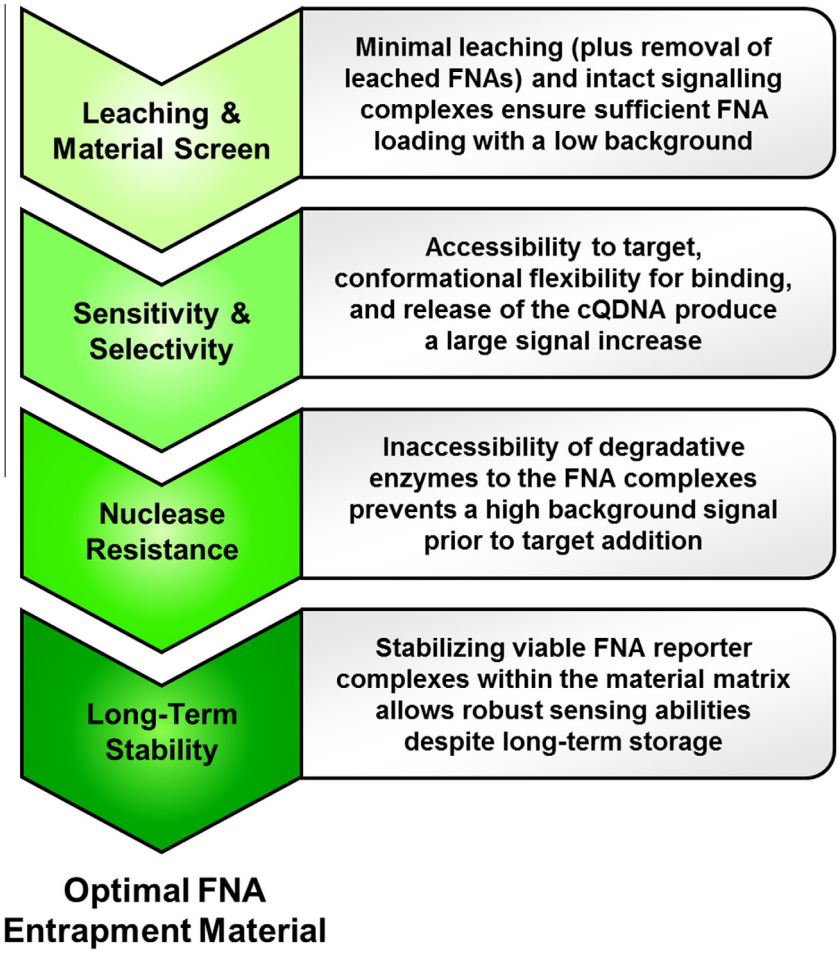

Fig. 3. Order of assays conducted for evaluating sol–gel entrapped FNA properties and performance.

enhancement is ~10% that of maximal cleavage as determined by PAGE due to quenching of fluorescence by the metal ions at higher concentrations [47]).

Analytes (3 μL at the appropriate concentration to obtain the final concentration listed) are either added directly to solution samples or the overlaying buffer of material samples after measuring initial baseline fluorescence (stock analyte solutions for the RNA aptamers are heated at 90 °C for 5 min and cooled to room temperature for 10 min prior to addition to ensure no RNase contamination).

3.4.3. Sensitivity and selectivity assays

Based on the results obtained from the initial material screen, one or a subset of materials that show superior performance in terms of total signal enhancements and/or response rates can be selected for more extensive evaluation of the entrapped FNA target-binding sensitivity and selectivity. Here, target concentration gradients for the appropriate FNA system, usually 0–200% the concentration used in the screen, are introduced to sol–gel entrapped FNAs and compared to data obtained in solution. From these data, the dynamic range and limit of detection can be calculated and compared from the fluorescence signal enhancements and initial rates.

To assess the selectivity of the entrapped FNA for their cognate target over structurally-related molecules, both native and mutant versions of the FNA complexes are immobilized in their optimal material and examined for fluorescence signal generation. Species used to test for selectivity are listed above in Section 2.2.2 and are added to wells containing the native FNA at their respective 100% concentrations, while the correct targets are added to wells containing the mutant constructs. In these studies, the endpoint fluorescence can be compared to that of the appropriate target (at its 100% concentration) with its respective FNA.

3.4.4. Nuclease degradation studies

To examine the protective effects of entrapping FNA reporters, a comparison of FNA stability (i) in solution, (ii) immobilized by a biotinylated 5′-end in a streptavidin coated microwell, and (iii) entrapped within its optimal sol–gel derived material, when in the presence of appropriate nucleases should be performed. In studies involving functional DNA, DNase I is used since it is an endonuclease that digests both single- and double-stranded DNA [48]. For RNA species, RNase A is a good choice due to its abundance in biological fluids [49], while RNase H is known to degrade RNA from RNA/DNA hybrids [50] such as the tripartite reporter complex. Degradation by these nucleases can be monitored through an increase in fluorescence intensity as the distance between the fluorescein and dabcyl moieties increases due to release of the cQDNA, cFDNA or both from the digested FNA species.

Solution-phase and entrapped FNAs can be prepared as described above; while immobilization on streptavidin coated plates is performed as described by the manufacturer (FNA sequences can easily be synthesized and ordered with terminally-bound biotin moieties to attach to the plate surface). The FNA complexes are treated with equimolar amounts (3 units) of DNAse I, RNase A, or RNase H by direct addition to solution samples or the overlaying buffer of material samples after measuring

initial baseline fluorescence (similar to the material screen/target-binding fluorescence measurements).

3.4.5. Long-term stability assays

The subset of optimal sol–gel derived materials doped with their respective FNA species can be prepared and aged as described above. These materials should be overlaid with at least 100 μL buffer and the 96-microwell plates covered with lids and wrapped in Parafilm to prevent evaporation upon storage. Plates are stored for up to 1 month at 4 °C in the dark prior to target-binding measurements. Buffered solutions containing the FNA reporter complexes can be prepared in microcentrifuge tubes and stored in the dark at 4 °C for comparison. Following the appropriate storage time, the materials in the plates are washed to remove any leached materials (as in Section 3.4.1) or aliquots of the solutions are put in plates and assessed for their target-binding response as in Section 3.4.2.

3.4.6. Co-entrapment assays

Using fluorescence signaling FNAs to monitor the catalytic activity of a protein enzyme can also be performed by co-entrapping these two species. In our co-entrapment study [42], the conversion of adenosine to inosine by the enzyme ADA is monitored by the ATP-binding aptamer, which also binds adenosine (but shows no affinity for inosine). When active ADA and aptamer are together, adenosine depletes rapidly and the aptamer signal decreases with time. However, when ADA is inhibited by EHNA, the aptamer reporter remains fluorescent with the high concentration of adenosine present. The aptamer and ADA are either co-entrapped in a single phase or segregated by separate material layers with the enzyme on top of the aptamer layer.

The mixed system is prepared with ADA and aptamer at final concentrations of 125 nM and 60 nM, respectively, in DNA aptamer assay buffer mixed with SS in a 1:1 (v/v) ratio to form a 2.3 mm thick monolith. The layered system is prepared by combining a buffered solution of aptamer (120 nM final concentration) with SS to form the first ~1.1 mm thick layer, which is allowed to gel and age for 1 h prior to the addition of a second layer containing 250 mM ADA entrapped in SS (so that the total concentrations amount to that of the mixed system). Each final material, single-phase or top layer, is allowed to gel and age for 2 h prior to addition of the buffer overlay. Assays are performed by first adding 15 different concentrations of EHNA (one per well), spanning the expected IC_{50} value of 100 nM (derived from literature K_I of 6.5 nM [51]), to the buffer overlay and incubating for 60 min. Following inhibitor incubation, 1 mM final concentration of adenosine is added and the fluorescence monitored over time as in experiments listed above.

In both cases, the data are normalized and the fluorescence response plotted against inhibitor concentration, with the most consistent IC_{50} values obtained by integrating the area under the response curve (as opposed to using endpoint intensity or slope of the curve). These IC_{50} values are determined by fitting the data to the Hill equation, using Sigma Plot graphing software and K_I values can be derived from the IC_{50} plots using the equation [52]:

$$K_I = IC_{50}/([S]/K_M + 1) \quad (1)$$

where $[S]$ is the substrate concentration and K_M is the Michaelis constant for the enzyme and substrate.

4. Results and discussion

4.1. Evaluating the materials screen

The time-dependent target-binding response data can be used to compare the degree and rate of signal enhancement in the various materials with solution. For example, Fig. 4 shows that the greatest enhancements and rates of signal development for the tripartite ATP-binding DNA aptamer were obtained after entrapment in DGS and SS. In our other studies assessing the entrapment of DNAzymes or RNA aptamer reporters, optimal performance was observed when using composite materials with 40% MTMS (in 60% TMOS), demonstrating that different types of FNA reporters may require a different optimal material (although only polar materials were tested in the study involving DNA aptamers so their function in composite materials is currently unknown). Generally, a slight reduction in the response time of entrapped FNAs is expected due to diffusional barriers to mass transport of the analyte through the silica matrix. However, mass transport limitations can be minimized by reducing the volume of the material through which the analyte must travel to reach entrapped FNAs by, for example, employing thin films [53].

Evaluating the un-normalized data from the materials screen allows for discrimination of a few factors that could affect the performance of the entrapped FNA species. Firstly, a very low initial fluorescence may be caused by a high amount of leaching, which can be correlated to the results of the leaching experiments. In all our studies, leaching demonstrated the general trend of increased leaching with increased hydrophobicity and pore size of the material, with the overall degree of leaching being relatively high compared to proteins [54]. Despite this, it was found that even materials with up to 30% leaching can still provide sufficient signal enhancements upon target introduction.

Observing a high initial fluorescence background may be due to reduced quenching due to cFDNA and/or cQDNA dehybridization upon entrapment. It is important to ascertain the expected decrease and increase in fluorescence signal, upon cQDNA or target addition, respectively, for the FNA reporters in solution for ease of comparison to entrapped species at the same concentration after accounting for leaching. Assessing the emission intensity of entrapped FNA complexes with cQDNA to those without can also aid in interpreting dehybridization upon entrapment. For example, using the tripartite ATP-binding aptamer, the quenching efficiency of the reporter in solution is greater than 12-fold in the presence of cQDNA, however, in comparing the background intensities of the entrapped cFDNA-aptamer system with the tripartite complex containing cQDNA, only a 10-fold decrease in fluorescence is observed [39]. Thus, the lower quenching efficiency when entrapped leads to the decreased signal potential upon binding target

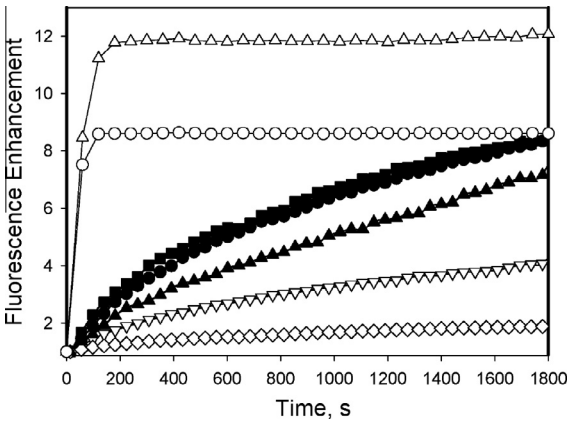

Fig. 4. Screening various materials for optimal performance of the ATP-binding DNA aptamer. Fluorescence signal enhancements of the tripartite aptamer upon addition of 2 mM ATP in solution (△), or entrapped in different sol–gel derived materials: DGS (■), DGS + 0.1% APTES (◇), SS (●), SS + 0.1% APTES (▽), and TEOS (▲). The signal enhancement for the bipartite aptamer in solution (○) is also shown. Figure adapted from [39].

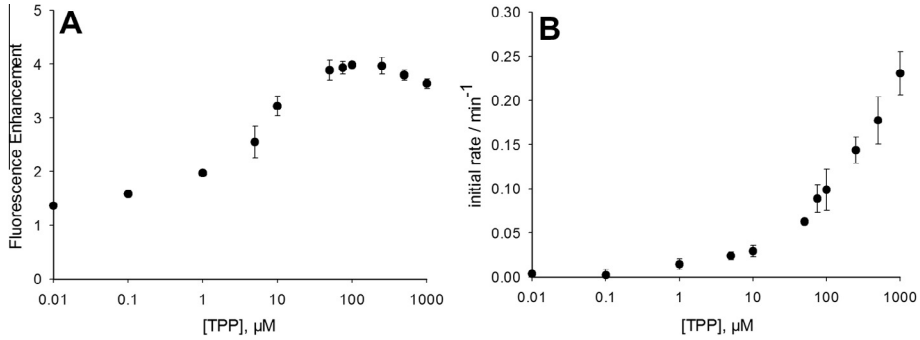

Fig. 5. Concentration-dependent response curves of entrapped TPP-binding RNA aptamer using (A) normalized fluorescence signal enhancement or (B) changes in initial rate of response. Data adapted from [41].

(observed in Fig. 4). Generally, the fold quenching of any reporter system should be at least 1.2× the expected final signal enhancement. The use of the *cis*-acting DNAzyme construct and bipartite DNA aptamer complex may help to eliminate any false signaling arising from substrate or cFDNA dehybridization, respectively; however, such bipartite designs for RNA aptamers are more difficult and expensive to create (as this cannot be done through *in vitro* transcription). Moreover, moving the fluorophore to the aptamer strand may increase its distance from the quencher moiety, slightly increasing background fluorescence and lowering the potential target-binding signal enhancement (due to the sensitive Förster distance dependence involved in energy transfer systems), as seen in Fig. 4.

If the background intensity is low but little to no signal enhancement is observed upon addition of target, the FNA may be inaccessible to the externally added target molecules or may not have enough conformational flexibility to undergo the structural change for target binding and signaling. In either case, hindrance of the target binding or signaling of the entrapped FNA reporter is indicative of a poor material for this FNA entrapment.

4.2. FNA performance in optimal materials

Using the optimal materials found in the screen, the target concentration-dependent signal enhancements of the entrapped FNAs should be tested for to ensure that the sensitivity, detection limit and dynamic range is equivalent to the values reported in solution. An advantage of using kinetic measurements when evaluating entrapped FNA sensitivity is the ability to assess the rate of response, which has proven to be useful in broadening the dynamic range of detection. For example, Fig. 5 compares the endpoint fluorescence signal enhancement with the initial rate responses for TPP detection using an RNA aptamer reporter. While both methods of analysis provide a detection limit of 1 μM, the use of initial rate data offers a dynamic range 20× greater than that using the fluorescence signal enhancement only. A combination of analysis methods may prove advantageous for certain applications that require an extended dynamic range.

Selectivity of each entrapped FNA reporter should also be similar to that observed in solution in order to demonstrate that the integrity of binding/catalytic site was not compromised upon entrapment. Retaining the selectivity of the signaling FNAs can be exploited to produce microwell plate-based multiplex assays by adding FNAs for different targets to different wells in a single plate.

Fluorimaging of the entire plate can then be performed to quickly determine target binding "hits" as demonstrated by comparing the response of the three metal ion-sensing DNAzymes in two different materials upon introduction of various metals

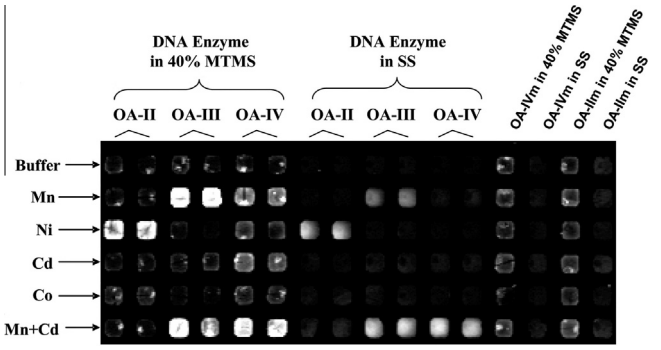

Fig. 6. Fluorimage of a 384-well plate with three different metal ion-sensing DNAzymes entrapped in two different materials, taken after the addition of various divalent metal ions (or buffer). Figure adapted from [40].

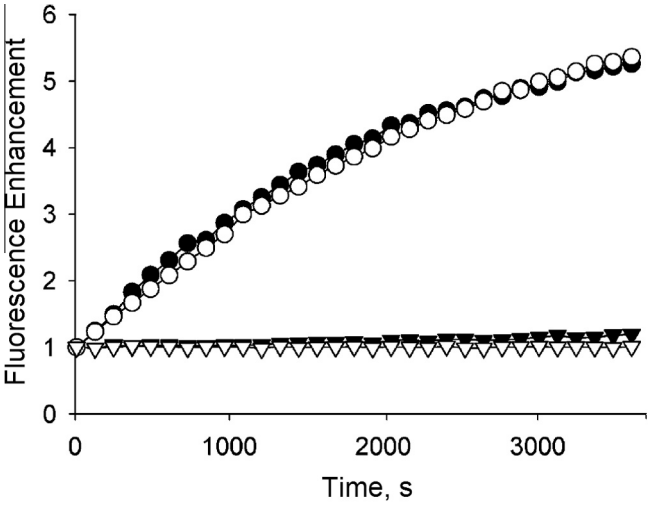

Fig. 7. Changes in fluorescence signal of the ATP-binding aptamer upon exposure to DNase in different conditions: aptamer in solution (●), aptamer immobilized on streptavidin-coated microtiter wells (○), aptamer entrapped in SS (▼), and DNase-free control (▽). Figure adapted from [39].

(Fig. 6). In this example, mutant constructs (uncleavable versions of DNAzymes with similar leaching and quenching behavior) were used for blank subtraction and placed in wells alongside the samples for simple on-array background correction from a single image. Upon addition of different divalent ions singly or in mixtures, the entrapped DNAzymes produced the expected pattern of response: OA-II fluoresced only with Ni(II), OA-III revealed the

presence of Mn(II) either alone or in the presence of Cd(II) and OA-IV required both Mn(II) and Cd(II) for maximal signal enhancement. No false signaling occurred from any DNAzyme in the presence of non-binding metal ions such as Co(II). Qualitatively, the samples based on 40% MTMS are much brighter than those derived from SS (although mutant samples in this material also showed greater brightness) and quantitative analysis of the pixel intensity in each well reveals that the DNAzymes entrapped in 40% MTMS indeed present a greater fold increase in fluorescence even after mutant blank correction. Importantly, these results show that ionic species such as metal ions can permeate through the anionic silica matrix (presumably owing to the high ionic strength of the test buffer) and that the entrapped DNAzymes are able to retain catalytic function and displace the F and Q moieties sufficiently to produce a useable fluorescence signal.

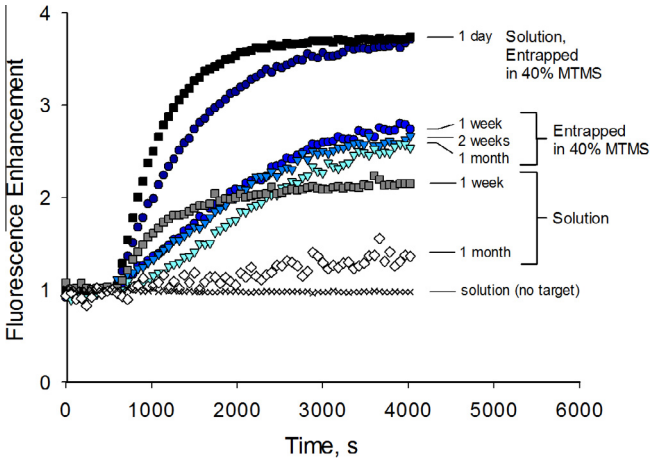

Fig. 8. Fluorescence signaling ability of solution-based or sol–gel entrapped TPP-binding RNA aptamer after increasing storage time (using 100 μM TPP). Adapted from [41].

The key advantage of entrapping FNAs within a sol–gel derived matrix, relative to more common covalently and affinity based immobilization methods, is that it can provide a steric barrier to entry of digestive enzymes that can degrade the FNA. This can be observed in Fig. 7, with the entrapped DNA aptamer reporter for ATP detection undergoing only a minor change in fluorescence intensity upon addition of DNase I. On the other hand, both the FNAs in solution and those surface-immobilized via a streptavidin–biotin linkage showed a drastic increase in fluorescence intensity due to dequenching upon degradation, demonstrating failure to provide any protection from nuclease digestion. It should be noted, however, that while nuclease exclusion from the material is a great advantage in developing solid-phase FNA biosensors, the inherent nature of FNA entrapment and retention within mesoporous sol–gel derived materials makes this method unsuitable for the detection of high molecular weight analytes (such as proteins or cells) that also cannot penetrate the pores of the material in order to interact with the entrapped FNA. Therefore, this method is limited to small molecule detection, which is serendipitously an area where elicitation of monoclonal antibodies is difficult.

The benefit of protection from degradation is again highlighted by long-term stability studies involving the fluorescence signaling version of a naturally-occurring RNA aptamer for the detection of TPP (Fig. 8). The signaling capacity of these RNA aptamers in solution significantly decreases over time with minimal (less than 1.5×) signal enhancements upon target addition after one month of storage, due to high fluorescence background signals caused by dequenching during degradation. However, entrapped RNA aptamers only exhibited a slight loss of activity (~20–30%) over the 1 month timespan. The loss in signal most likely does not represent degradation but reflects continued evolution of the sol–gel matrix, leading to pore shrinkage and restriction of either dynamic motion (thus an inability to structure-switch) or target access to the entrapped FNA [55]. Nevertheless, retention of adequate signaling ability after long-term storage is essential in developing robust solid-phase sensors, particularly when using labile species such as RNA aptamers that tend to suffer great susceptibility to degradation.

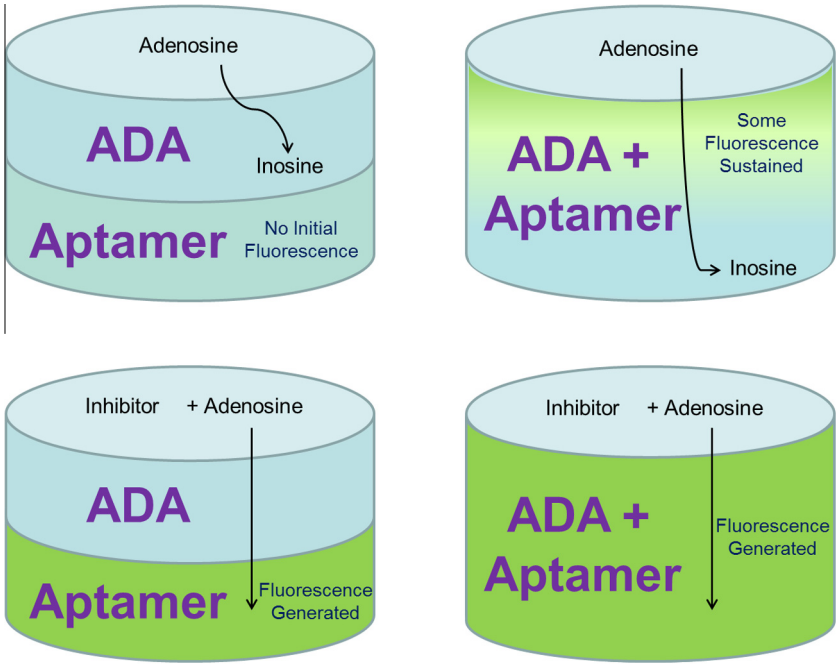

Fig. 9. Schematic of our aptamer–enzyme co-entrapment study using a stacked two-layer monolith approach with ADA above the aptamer layer (left) or a single mixed component monolith (right).

4.3. Co-entrapment assays

An advantage of sol–gel-based materials is their ability to entrap a wide range of biological species, including protein and FNA. More importantly, we demonstrated that such material could be used to separating enzymes and aptamer reporters into distinct layers, providing a means to control sequential reactions and ultimately generate more accurate IC_{50} and K_I values for inhibition assay than when the enzyme and aptamer reporter were entrapped together (or used together in solution). This result is due to the ability of the enzyme to establish equilibrium in the upper layer so that its catalytic rate determines the level of substrate exposure in the subsequent aptamer layer. When both biomolecules were co-entrapped in a single layer, target/substrate interacting with aptamer species near the top of the material generated a higher background fluorescence signal than in the case where aptamers were restricted to the bottom material layer (Fig. 9). However, if the aptamer is selected for the product of a reaction, it is likely that co-entrapment in a single layer may provide a more accurate assessment of inhibitor potency since the issue of the enzyme and FNA competing for the same substrate at the same time will not exist.

Moreover, this study demonstrates the ability for spatial separation of coupled assays in unique solid-phase sensor schemes that can offer advantages when biomolecules are (i) incompatible (e.g. FNAs and a nuclease), (ii) require different conditions (such as a different matrix environment or reagents) to function, or (iii) need varying reaction times (i.e., for multiple assay steps or pre-incubation), using a simple methodology.

5. Concluding remarks

A simple and general approach for immobilizing and improving the stability of viable fluorescence-signaling FNAs is demonstrated based on their entrapment in sol–gel derived materials. Our studies have shown that all the different classes of signaling FNA can be entrapped within optimized sol–gel derived material, demonstrating only moderate leaching with sensitivity, selectivity and signaling capabilities similar to the same FNAs free in solution. Entrapment also resulted in protection of the various FNAs against degradation from nucleases, improving their long-term stability and potential for *in vivo* sensing. This immobilization scheme expands the use of FNA reporter systems in practical solid-phase biosensor technology, including multiplexed target-detection assays and enzyme inhibitor screens (using FNA/enzyme co-entrapment).

Importantly, sol–gel derived materials possess significant versatility in that they are amenable to many configurations, particularly as thin-film coatings for interfacing to a variety of analytical devices, such as electrodes and optical fibers [38,56]. Although the studies presented focus on fluorescence signaling, the use of the sol–gel method for biomolecular entrapment has been employed in both colorimetric and electrochemical sensor formats [57] and thus presents a broadly applicable platform for preparing solid-phase FNA-based sensors.

Acknowledgements

Funding for this work was provided by the Natural Sciences and Engineering Research Council of Canada (NSERC) and the SENTINEL Bioactive Paper Network. We thank Pui Sai Lau, Yutu Shen, Gillian Mackey, Darin Gloster, Dr. Nicholas Rupcich, Dr. Razvan Nutiu, Dr. William Chiuman and Professor Yingfu Li for their contributions to this work. J.D.B holds the Canada Research Chair in Bioanalytical Chemistry and Biointerfaces.

References

[1] J. Liu, Z. Cao, Y. Lu, Chem. Rev. 109 (2009) 1948–1998.
[2] R.R. Breaker, Curr. Opin. Chem. Biol. 1 (1997) 26–31.
[3] A.D. Ellington, J.W. Szostak, Nature 346 (1990) 818–822.
[4] C. Tuerk, L. Gold, Science 249 (1990) 505–510.
[5] D.L. Robertson, G.F. Joyce, Nature 344 (1990) 467–468.
[6] D.P. Bartel, J.W. Szostak, Science 261 (1993) 1411–1418.
[7] J.F. Lee, J.R. Hesselberth, L.A. Meyers, A.D. Ellington, Nucleic Acids Res. 32 (2004) D95–100.
[8] G.M. Emilsson, R.R. Breaker, Cell. Mol. Life Sci. 59 (2002) 596–607.
[9] S.K. Silverman, Org. Biomol. Chem. 2 (2004) 2701–2706.
[10] K. Kruger, P.J. Grabowski, A.J. Zaug, J. Sands, D.E. Gottschling, T.R. Cech, Cell 31 (1982) 147–157.
[11] C. Guerrier-Takada, K. Gardiner, T. Marsh, N. Pace, S. Altman, Cell 35 (1983) 849–857.
[12] W. Winkler, A. Nahvi, R.R. Breaker, Nature 419 (2002) 952–956.
[13] W.C. Winkler, R.R. Breaker, ChemBioChem 4 (2003) 1024–1032.
[14] S.D. Jayasena, Clin. Chem. 45 (1999) 1628–1650.
[15] N.K. Navani, Y.F. Li, Curr. Opin. Chem. Biol. 10 (2006) 272–281.
[16] S.P. Song, L.H. Wang, J. Li, J.L. Zhao, C.H. Fan, TrAC, Trends Anal. Chem. 27 (2008) 108–117.
[17] K.A. Marshall, A.D. Ellington, Methods Enzymol. 318 (2000) 193–214.
[18] M. Oivanen, S. Kuusela, H. Lonnberg, Chem. Rev. 98 (1998) 961–990.
[19] Y. Li, R.R. Breaker, J. Am. Chem. Soc. 121 (1999) 5364–5372.
[20] G.A. Soukup, R.R. Breaker, RNA 5 (1999) 1308–1325.
[21] R. Nutiu, Y. Li, J. Am. Chem. Soc. 125 (2003) 4771–4778.
[22] P.S. Lau, B.K. Coombes, Y. Li, Angew. Chem., Int. Ed. 49 (2010) 7938–7942.
[23] S.W. Santoro, G.F. Joyce, Biochemistry 37 (1998) 13330–13342.
[24] R.P. Cruz, J.B. Withers, Y. Li, Chem. Biol. 11 (2004) 57–67.
[25] S.H.J. Mei, Z.J. Liu, J.D. Brennan, Y.F. Li, J. Am. Chem. Soc. 125 (2003) 412–420.
[26] W. Chiuman, Y. Li, J. Mol. Biol. 357 (2006) 748–754.
[27] W. Chiuman, Y. Li, Nucleic Acids Res. 35 (2007) 401–405.
[28] I. Willner, B. Shlyahovsky, M. Zayats, B. Willner, Chem. Soc. Rev. 37 (2008) 1153–1165.
[29] R.A. Potyrailo, R.C. Conrad, A.D. Ellington, G.M. Hieftje, Anal. Chem. 70 (1998) 3419–3425.
[30] G. Ramsay, Nat. Biotechnol. 16 (1998) 40–44.
[31] S. Balamurugan, A. Obubuafo, S.A. Soper, D.A. Spivak, Anal. Bioanal. Chem. 390 (2008) 1009–1021.
[32] J.D. Andrade, V. Hlady, A.P. Wei, Pure Appl. Chem. 64 (1992) 1777–1781.
[33] H.H. Weetall, Appl. Biochem. Biotechnol. 41 (1993) 157–188.
[34] R.J. White, N. Phares, A.A. Lubin, Y. Xiao, K.W. Plaxco, Langmuir 24 (2008) 10513–10518.
[35] S. Braun, S. Rappoport, R. Zusman, D. Avnir, M. Ottolenghi, Mater. Lett. 10 (1990) 1–5.
[36] R.B. Bhatia, C.J. Brinker, A.K. Gupta, A.K. Singh, Chem. Mater. 12 (2000) 2434–2441.
[37] D. Avnir, S. Braun, O. Lev, M. Ottolenghi, Chem. Mater. 6 (1994) 1605–1614.
[38] J.D. Brennan, Acc. Chem. Res. 40 (2007) 827–835.
[39] N. Rupcich, R. Nutiu, Y. Li, J.D. Brennan, Anal. Chem. 77 (2005) 4300–4307.
[40] Y.T. Shen, G. Mackey, N. Rupcich, D. Gloster, W. Chiuman, Y.F. Li, J.D. Brennan, Anal. Chem. 79 (2007) 3494–3503.
[41] C. Carrasquilla, P.S. Lau, Y. Li, J.D. Brennan, J. Am. Chem. Soc. 134 (2012) 10998–11005.
[42] N. Rupcich, R. Nutiu, Y.F. Li, J.D. Brennan, Angew. Chem., Int. Ed. 45 (2006) 3295–3299.
[43] R. Nutiu, Y. Li, Methods 37 (2005) 16–25.
[44] M.A. Brook, Y. Chen, K. Guo, Z. Zhang, J.D. Brennan, J. Mater. Chem. 14 (2004) 1469–1479.
[45] M.A. Brook, Y. Chen, K. Guo, Z. Zhang, W. Jin, A. Deisingh, J. Cruz-Aguado, J.D. Brennan, J. Sol–Gel Sci. Technol. 31 (2004) 343–348.
[46] T.R. Besanger, Y. Chen, A.K. Deisingh, R. Hodgson, W. Jin, S. Mayer, M.A. Brook, J.D. Brennan, Anal. Chem. 75 (2003) 2382–2391.
[47] N. Rupcich, W. Chiuman, R. Nutiu, S. Mei, K.K. Flora, Y.F. Li, J.D. Brennan, J. Am. Chem. Soc. 128 (2006) 780–790.
[48] N. Kienzle, D. Young, S. Zehntner, G. Bushell, T.B. Sculley, Biotechniques 20 (1996) 612–616.
[49] R.T. Raines, Chem. Rev. 98 (1998) 1045–1066.
[50] H. Donis-Keller, Nucleic Acids Res. 7 (1979) 179–192.
[51] R.P. Agarwal, Pharmacol. Ther. 17 (1982) 399–429.
[52] Y. Cheng, W.H. Prusoff, Biochem. Pharmacol. 22 (1973) 3099–3108.
[53] K. Flora, J.D. Brennan, Analyst 124 (1999) 1455–1462.
[54] L. Zheng, W.R. Reid, J.D. Brennan, Anal. Chem. 69 (1997) 3940–3949.
[55] T. Keeling-Tucker, J.D. Brennan, Chem. Mater. 13 (2001) 3331–3350.
[56] M.R.N. Monton, E.M. Forsberg, J.D. Brennan, Chem. Mater. 24 (2011) 796–811.
[57] D. Avnir, T. Coradin, O. Lev, J. Livage, J. Mater. Chem. 16 (2006) 1013–1030.